Engineered swift equilibration of a Brownian particle

Ignacio A. Martínez[1], Artyom Petrosyan[1], David Guéry-Odelin[2], Emmanuel Trizac[3] and Sergio Ciliberto[1]*

A fundamental and intrinsic property of any device or natural system is its relaxation time τ_{relax}, which is the time it takes to return to equilibrium after the sudden change of a control parameter[1]. Reducing τ_{relax} is frequently necessary, and is often obtained by a complex feedback process. To overcome the limitations of such an approach, alternative methods based on suitable driving protocols have been recently demonstrated[2,3], for isolated quantum and classical systems[4–9]. Their extension to open systems in contact with a thermostat is a stumbling block for applications. Here, we design a protocol, named Engineered Swift Equilibration (ESE), that shortcuts time-consuming relaxations, and we apply it to a Brownian particle trapped in an optical potential whose properties can be controlled in time. We implement the process experimentally, showing that it allows the system to reach equilibrium 100 times faster than the natural equilibration rate. We also estimate the increase of the dissipated energy needed to get such a time reduction. The method paves the way for applications in micro- and nano-devices, where the reduction of operation time represents as substantial a challenge as miniaturization[10].

The concepts of equilibrium and of transformations from an equilibrium state to another, are cornerstones of thermodynamics. A textbook illustration is provided by the expansion of a gas, starting at equilibrium and expanding to reach a new equilibrium in a larger vessel. This operation can be performed either very slowly by a piston, without dissipating energy into the environment, or alternatively quickly, letting the piston freely move to reach the new volume. In the first case, the transformation takes a long (virtually infinite) time to be completed, while the gas is always in a quasi-equilibrium state. In the second case instead, the transformation is fast but the gas takes its characteristic relaxation time τ_{relax} to reach the new equilibrium state in the larger volume. This is the time required for the exploration of the new vessel. More generally, once a control parameter is suddenly changed, the accessible phase space changes too[1,11]; the system adjusts and needs a finite time to reach the final equilibrium distribution. This equilibration process of course plays a key role in out-of-equilibrium thermodynamics.

An important and relevant question related to optimization theory is whether a targeted statistical equilibrium state can be reached in a chosen time, arbitrarily shorter than τ_{relax}. Such strategies are reminiscent of those worked out in the recent field of shortcut to adiabaticity[2,3]; they aim at developing protocols, both in quantum and in classical regimes, allowing the system to move as fast as possible from one equilibrium position to a new one, provided
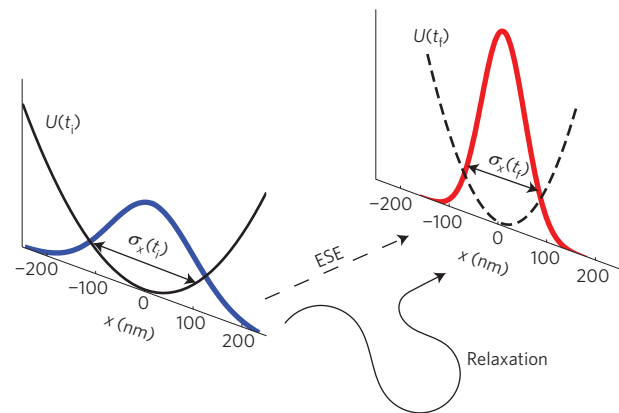

Figure 1 | Sketch of the process. At initial time t_i, the particle is at equilibrium, confined in a potential of stiffness κ_i (black line), and $\rho(x)$ (blue histogram) has variance $\sigma_x^2(t_i) = k_B T/\kappa_i$. After a long relaxation where κ is gradually increased, the particle is at time t_f at equilibrium in a stiffer potential (dashed black line). As $\kappa_f > \kappa_i$, the variance $\sigma_x^2(t_f)$ of position (red histogram) is smaller than its initial counterpart. The goal is to work out a protocol with a suitable dynamics $\kappa(t)$ that would ensure equilibrium at an arbitrary chosen final time t_f, no matter how small.

that there exists an adiabatic transformation relating the two[12–14]. So far, proof-of-principle experiments have been carried out for isolated systems[4–9] and for photonics circuit design[15–18]. Yet, the problem of open classical systems is untouched. Here, we solve this question by putting forward an accelerated equilibration protocol for a system in contact with a thermal bath. Such a protocol shortcuts quasi-stationarity, according to which a driven open system remains in equilibrium with its environment at all times. This is a key step for a number of applications in nano-oscillators[19], in the design of nanothermal engines[20], or in monitoring mesoscopic chemical or biological processes[21], for which thermal fluctuations are paramount and an accelerated equilibration desirable for improved power. We dub the method Engineered Swift Equilibration (ESE).

However, an arbitrary reduction of the time to reach equilibrium will have unavoidable consequences from an energetical point of view[22]. The question of the corresponding cost is relevant as such, but also for applications, for example in nano-devices[10], where the goal is the reduction in size and execution time of a given process. Here, beyond the theoretical derivation of the procedure, we develop an experimental demonstration of ESE, studying the dynamics of

[1]Laboratoire de Physique, CNRS UMR5672 Université de Lyon, École Normale Supérieure, 46 Allée d'Italie, 69364 Lyon, France. [2]Laboratoire Collisions Agrégats Réactivité, CNRS UMR5589, Université de Toulouse, 31062 Toulouse, France. [3]LPTMS, CNRS, Univ. Paris-Sud, Université Paris-Saclay, 91405 Orsay, France. *e-mail: sergio.ciliberto@ens-lyon.fr
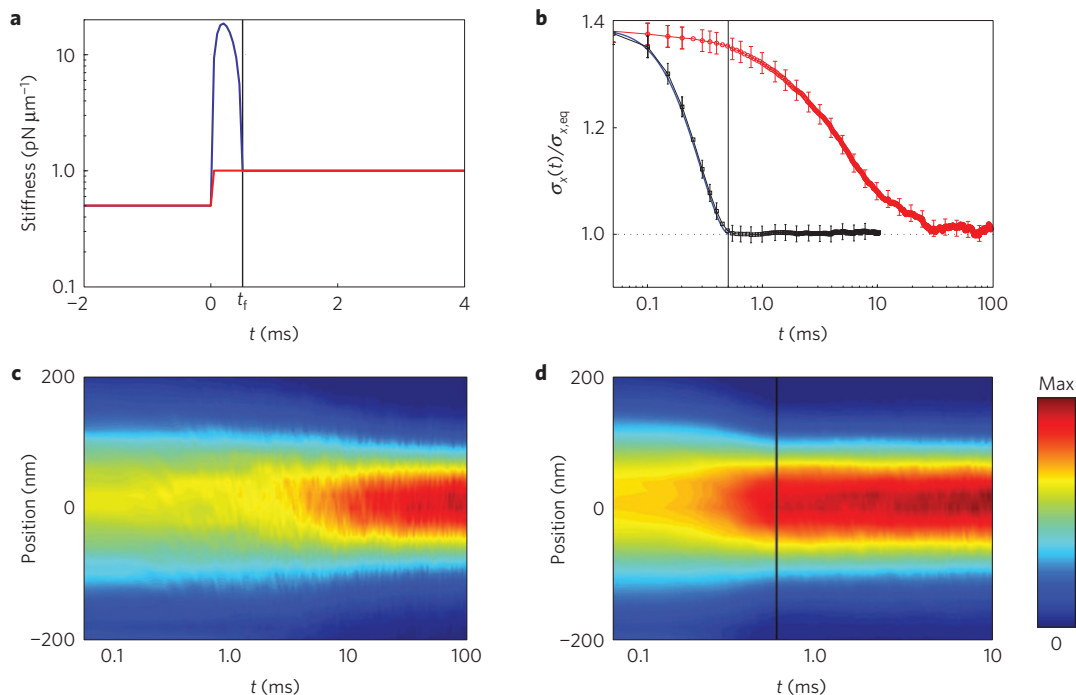
843

Figure 2 | Dynamics of the system along the STEP and ESE protocol. a, Experimental protocols: STEP route (red) and ESE route (blue). The system starts with $\kappa_i = 0.5\,\mathrm{pN\,\mu m^{-1}}$ at $t = 0$ to finish with $\kappa_f = 1.0\,\mathrm{pN\,\mu m^{-1}}$. In all figures, the vertical solid line at $t = t_f$ indicates the end of the ESE protocol. **b**, Normalized standard deviation $\sigma_x(t)$ of the particle's trajectory along the STEP (red circles) and ESE protocol (black squares). The blue solid line represents the theoretical prediction of the variance evolution, that is, $1/(2\alpha)$, where α is given by equation (7). The error bars take into account the calibration and the statistical errors. **c**, Time evolution of the position pdf. The colour map of $\rho(x, t)$ is plotted after an instantaneous change of the stiffness at $t = 0$ (STEP). **d**, ESE counterpart of panel **c**.

a colloidal particle in an optical potential. The energetics of the system will also be analysed in depth, shedding light on the inherent consequences of timescale reduction[22–27].

Our experimental system consists of a microsphere immersed in water[28] (see Methods). The particle is trapped by an optical harmonic potential $U(x, t) = \kappa(t)x^2/2$, where x is the particle position and $\kappa(t)$ is the stiffness of the potential, which can be controlled by the power of the trapping laser[20]. The system is affected by thermal fluctuations; its dynamics is overdamped and described by a Langevin equation. Our Brownian particle has a relaxation time defined as $\tau_{\mathrm{relax}} = \gamma/\kappa$, where γ is the fluid viscous coefficient. At equilibrium, the probability density function (pdf) $\rho(x)$ of x is Gaussian $\rho_{\mathrm{eq}}(x) = 1/\sqrt{\pi\sigma_x^2}\exp(-x^2/(2\sigma_x^2))$, with variance $\sigma_x^2 = k_B T/\kappa$, as prescribed by the equipartition theorem. Here, k_B is the Boltzmann constant and T the bath temperature. In this system, we consider the compression process sketched in Fig. 1, in which the stiffness is changed from an initial value to a larger one. The evolution of the system during the relaxation towards the new equilibrium state is monitored through the position pdf $\rho(x, t)$, which is Gaussian at all times (see Methods and Supplementary Information). Thus, the distribution $\rho(x, t)$ is fully characterized by the time evolution of its mean and its standard deviation $\sigma_x(t)$. The main question is now that of finding, provided it exists, a suitable time evolution of the stiffness $\kappa(t)$ (our control parameter), for which the equilibration process is much faster than τ_{relax}. This question can be affirmatively answered using a particular solution of the Fokker–Planck equation (see Methods and Supplementary Information). We emphasize that the ESE idea is not restricted to manipulating Gaussian states, and that non-harmonic potentials U can be considered, along the lines presented in the Supplementary Information.

In this Letter, two methods are compared. On the one hand, at a given instant $t_i = 0$, we suddenly change κ from the initial value

κ_i to the final value κ_f. During this protocol, referred to as STEP, the particle mean position does not change, whereas the spread σ_x equilibrates to the new value $\sqrt{k_B T/\kappa_f}$ in about 3 relaxation times $\tau_{\mathrm{relax}} = \gamma/\kappa_f$. On the other hand, following the ESE procedure, $\kappa(t)$ is modulated in such a way that σ_x is fully equilibrated at $t_f \ll \tau_{\mathrm{relax}}$. The protocol which meets our requirements is given by equation (8) (in Methods). In the experiment, we select $\kappa_i = 0.5\,\mathrm{pN\,\mu m^{-1}}$ and $\kappa_f = 1.0\,\mathrm{pN\,\mu m^{-1}}$ in such a way that $\tau_{\mathrm{relax}} \simeq 15\,\mathrm{ms}$. Furthermore, to have a well-defined separation between timescales, we choose $t_f = 0.5\,\mathrm{ms}$, which is roughly 100 times smaller than the thermalization time in the STEP protocol. Both protocols are shown in Fig. 2a, where we can appreciate the rather complex time dependence of the ESE control procedure. This is a necessity to allow for a quick evolution to the new equilibrium state. The faster the evolution (smaller t_f), the stiffer the transient confinement must be (the maximum stiffness reached in Fig. 2a is $37\kappa_i$). To study the evolution of $\rho(x, t)$ for the two protocols, we perform the following cycle. First, the particle is kept at κ_i for 50 ms to ensure proper equilibration. Then, at $t = 0$ ms we apply the protocol (either STEP or ESE) and $x(t)$ is measured for 10 ms in the case of ESE and 100 ms for STEP. Finally, the stiffness is set again to κ_i and this cycle is repeated N times. The evolution of $\sigma_x(t)$ for $t > 0$ is obtained by performing an ensemble average over $N = 2 \times 10^4$ cycles.

The results are shown in Fig. 2b, where $\sigma_x(t)$ is plotted as a function of time for the two protocols, from one equilibrium configuration to the other. It appears that the engineered system reaches the target spread precisely at t_f, and subsequently does not evolve. On the other hand, the STEP equilibration occurs after a time close to $3\tau_{\mathrm{relax}}$. Figure 2c,d represents the complete STEP and ESE dynamics of $\rho(x)$. The Gaussian feature is confirmed experimentally during ESE, even far from equilibrium, as the kurtosis is $\mathrm{Kurt}(x) = (3.00 \pm 0.01)$. The results of Fig. 2 clearly show the efficiency of ESE, driving the system into equilibrium in
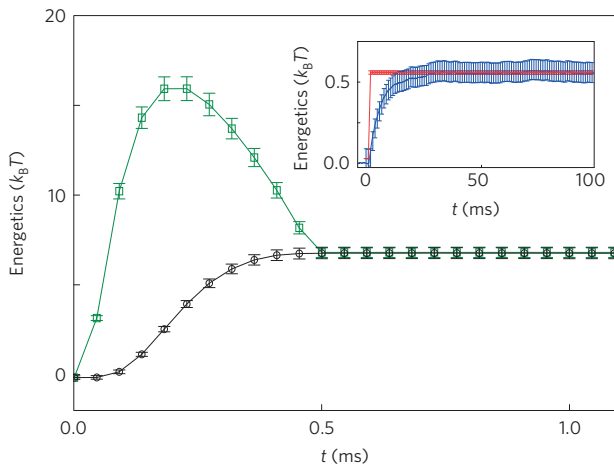
Figure 3 | Energetics of the ESE protocol. Average value of the cumulative work W (green squares) and heat Q (black circles) are represented as a function of time. The energy exchange stops within the protocol time $t_f = 0.5$ ms. For $t > t_f$, $\langle W \rangle = \langle Q \rangle$: the system is in an equilibrium steady state, in contact with an isothermal reservoir. Inset, energetics of the STEP protocol. Work (red curve) is exerted onto the system quasi-instantaneously, with an abrupt change of trap stiffness. On the other hand, heat (blue curve) is delivered along the whole equilibration process. The error bars, which take into account the calibration and the statistical errors, have the same relative value for ESE and STEP. Energy-wise, the ESE method seems more costly: this is the price for accelerating the thermalization process.

a time which is 100 times shorter than the nominal equilibration time $3\tau_{relax}$.

We now turn our attention to the energy required to achieve such a large time reduction. Developments in the field of stochastic thermodynamics[29] endow work W and heat Q with a clear mesoscopic meaning, from which a resolution better than $k_B T$ can be achieved experimentally (see Methods for an explicit definition). In Fig. 3, the complete energetics of our system is shown for the ESE and STEP protocols. The evolution of the mean cumulative work $\langle W(t) \rangle$ reveals the physical behaviour of the system undergoing ESE. In the first part of the protocol ($t < 0.2$ ms), confinement is increased, which provides positive work to the system. In the subsequent evolution ($0.2 < t < 0.5$ ms), work is delivered from the system to the environment through the decrease of the stiffness. In striking contrast to an adiabatic transformation, the value of heat increases monotonically, as the system dissipates heat all over the protocol. In the inset of Fig. 3, $\langle Q \rangle$ and $\langle W \rangle$ are shown for the STEP process. Notice how the work exerted on the system is almost instantaneous, whereas heat is delivered over a wide interval of time, up to complete equilibration. As expected, there is a price to pay for ESE. A significant amount of work is required to speed up the evolution and beat the natural timescale of our system[22]. It can be shown that the cost $\langle W(t_f) \rangle$ behaves like τ_{relax}/t_f for $t_f \to 0$. More precisely, this amounts to a time–energy uncertainty relation: $t_f \langle W(t_f) \rangle \sim 0.106 \, (2\tau_{relax}) \, k_B T$. If instead, one proceeds in a quasi-static fashion ($t_f \gg \tau_{relax}$), the cost reduces to the free energy difference, $k_B T \log(\kappa_f/\kappa_i)/2$, which is $0.35 \, k_B T$ when $\kappa_f = 2\kappa_i$. For the ESE experiments shown, we have $\langle W(t_f) \rangle \simeq 7.0 \, k_B T$, about twenty times larger.

Our results show the feasibility and expediency of accelerated protocols for equilibrating confined Brownian objects. The ESE path allows a gain of two orders of magnitude in the thermalization time, as compared to an abrupt change of control parameter (STEP process). The associated energetic cost has been assessed. Finally, although an overdamped problem has been solved here, the generalization of the ESE protocol to non-isothermal regimes for underdamped systems can in principle be worked out theoretically. Its application to AFM tips, vacuum optical traps, or to transitions between non-equilibrium steady states, constitutes a timely experimental challenge in this emerging field.

Methods

Methods, including statements of data availability and any associated accession codes and references, are available in the online version of this paper.

References

1. Boltzmann, L. *Lectures on Gas Theory* (Univ. California Press, 1964).
2. Torrontegui, E. *et al*. Shortcuts to adiabaticity. *Adv. At. Mol. Opt. Phys.* **62,** 117–169 (2013).
3. Deffner, S., Jarzynski, C. & del Campo, A. Classical and quantum shortcuts to adiabaticity for scale-invariant driving. *Phys. Rev. X* **4,** 021013 (2014).
4. Couvert, A., Kawalec, T., Reinaudi, G. & Guéry-Odelin, D. Optimal transport of ultracold atoms in the non-adiabatic regime. *Europhys. Lett.* **83,** 13001 (2008).
5. Schaff, J.-F., Song, X.-L., Vignolo, P. & Labeyrie, G. Fast optimal transition between two equilibrium states. *Phys. Rev. A* **82,** 033430 (2010).
6. Schaff, J.-F., Song, X.-L., Capuzzi, P., Vignolo, P. & Labeyrie, G. Shortcut to adiabaticity for an interacting Bose–Einstein condensate. *Europhys. Lett.* **93,** 23001 (2011).
7. Bason, M. G. *et al*. High-fidelity quantum driving. *Nature Phys.* **8,** 147–152 (2012).
8. Bowler, R. *et al*. Coherent diabatic ion transport and separation in a multizone trap array. *Phys. Rev. Lett.* **109,** 080502 (2012).
9. Walther, A. *et al*. Controlling fast transport of cold trapped ions. *Phys. Rev. Lett.* **109,** 080501 (2012).
10. Peercy, P. S. The drive to miniaturization. *Nature* **406,** 1023–1026 (2000).
11. Maxwell, J. C. On the dynamical theory of gases. *Phil. Trans. R. Soc. Lond.* **157,** 49–88 (1867).
12. Chen, X. *et al*. Fast optimal frictionless atom cooling in harmonic traps: shortcut to adiabaticity. *Phys. Rev. Lett.* **104,** 063002 (2010).
13. Guéry-Odelin, D., Muga, J., Ruiz-Montero, M. & Trizac, E. Nonequilibrium solutions of the Boltzmann equation under the action of an external force. *Phys. Rev. Lett.* **112,** 180602 (2014).
14. Papoular, D. & Stringari, S. Shortcut to adiabaticity for an anisotropic gas containing quantum defects. *Phys. Rev. Lett.* **115,** 025302 (2015).
15. Tseng, S.-Y. & Chen, X. Engineering of fast mode conversion in multimode waveguides. *Opt. Lett.* **37,** 5118–5120 (2012).
16. Tseng, S.-Y. Robust coupled-waveguide devices using shortcuts to adiabaticity. *Opt. Lett.* **39,** 6600–6603 (2014).
17. Ho, C.-P. & Tseng, S.-Y. Optimization of adiabaticity in coupled-waveguide devices using shortcuts to adiabaticity. *Opt. Lett.* **40,** 4831–4834 (2015).
18. Stefanatos, D. Design of a photonic lattice using shortcuts to adiabaticity. *Phys. Rev. A* **90,** 023811 (2014).
19. Kaka, S. *et al*. Mutual phase-locking of microwave spin torque nano-oscillators. *Nature* **437,** 389–392 (2005).
20. Martínez, I. A. *et al*. Brownian Carnot engine. *Nature Phys.* **12,** 67–70 (2016).
21. Collin, D. *et al*. Verification of the Crooks fluctuation theorem and recovery of RNA folding free energies. *Nature* **437,** 231–234 (2005).
22. Cui, Y.-Y., Chen, X. & Muga, J. G. Transient particle energies in shortcuts to adiabatic expansions of harmonic traps. *J. Phys. Chem. A* http://dx.doi.org/10.1021/acs.jpca.5b06090 (2015).
23. Schmiedl, T. & Seifert, U. Optimal finite-time processes in stochastic thermodynamics. *Phys. Rev. Lett.* **98,** 108301 (2007).
24. Schmiedl, T. & Seifert, U. Efficiency at maximum power: an analytically solvable model for stochastic heat engines. *Europhys. Lett.* **81,** 20003 (2008).
25. Aurell, E., Gawedzki, K., Mejia-Monasterio, C., Mohayaee, R. & Muratore-Ginanneschi, P. Refined second law of thermodynamics for fast random processes. *J. Stat. Phys.* **147,** 487–505 (2012).
26. Acconcia, T. V., Bonança, M. V. S. & Deffner, S. Shortcuts to adiabaticity from linear response theory. *Phys. Rev. E* **92,** 042148 (2015).
27. Zheng, Y., Campbell, S., De Chiara, G. & Poletti, D. Cost of transitionless driving and work output. Preprint at http://arXiv.org/abs/1509.01882 (2016).
28. Neuman, K. C. & Block, S. M. Optical trapping. *Rev. Sci. Instrum.* **75,** 2787–2809 (2004).
29. Sekimoto, K. *Stochastic Energetics* Vol. 799 (Springer, 2010).

Author contributions

All authors contributed substantially to this work.

Additional information

Supplementary information is available in the online version of the paper. Reprints and permissions information is available online at www.nature.com/reprints. Correspondence and requests for materials should be addressed to S.C.

Competing financial interests

The authors declare no competing financial interests.

Methods

Experimental set-up. Silica microspheres of radius 1 μm were diluted in milliQ water to a final concentration of a few spheres per millilitre. The microspheres were inserted into a fluid chamber, which can be displaced in three dimensions by a piezoelectric device (Nanomax TS MAX313/M). The trap is realized using a near-infrared laser beam (Lumics, $\lambda = 980$ nm with maximum power 500 mW) expanded and injected through an oil-immersed objective (Leica, 63× NA 1.40) into the fluid chamber. The trapping laser power, which determines the trap stiffness, is modulated by an external voltage V_κ by means of a Thorlabs ITC 510 laser diode controller with a switching frequency of 200 kHz. V_κ is generated by a National Instrument card (NI PXIe-6663) managed by a custom-made Labview program. The detection of the particle position is performed using an additional HeNe laser beam ($\lambda = 633$ nm), which is expanded and collimated by a telescope and passed through the trapping objective. The forward-scattered detection beam is collected by a condenser (Leica, NA 0.53), and its back focal-plane field distribution projected onto a custom position sensitive detector (PSD from First Sensor with a bandpass of 257 kHz) whose signal is acquired at a sampling rate of 20 kHz with a NI PXIe-4492 acquisition board.

Energetics measurement. From the experimental observables, the stiffness κ and the particle position x, it is possible to infer the energetic evolution of our system within the stochastic energetics framework[29]. The notion of work W is related to the energy exchange stemming from the modification of a given control parameter—here the trap stiffness. Alternatively, heat Q pertains to the energy exchanged with the environment, either by dissipation or by Brownian fluctuations. The work $W(t)$ and dissipated heat $Q(t)$ are expressed as $W(t) = \int_0^t (\partial U/\partial \kappa) \circ (\mathrm{d}\kappa/\mathrm{d}t') \mathrm{d}t'$, $Q(t) = -\int_0^t (\partial U/\partial x) \circ (\mathrm{d}x/\mathrm{d}t') \mathrm{d}t'$, where $\circ$ denotes the Stratonovich integral and U is the potential energy. Under this definition, the first law reads as $\Delta U(t) = W(t) - Q(t)$, where $W(t), Q(t)$ and $\Delta U(t)$ are fluctuating quantities. Because T is fixed, both ESE and STEP processes share the same value $\langle \Delta U(t_f) \rangle = 0$ between the initial and the final state. As a consequence, we have $\langle W(t_f) \rangle = \langle Q(t_f) \rangle$.

ESE protocol for the harmonic potential. Although the idea is general (as discussed in Supplementary Information), we first start by a presentation applying the method to harmonic confinement. The dynamics of the system is then ruled by the Langevin equation

$$\dot{x} = -\frac{\kappa(t)}{\gamma} x + \sqrt{D}\,\xi(t) \tag{1}$$

where a dot denotes time derivative and x is for the position of the Brownian particle. The friction coefficient $\gamma = 6\pi\nu R$ is here constant, ν being the kinetic viscosity coefficient and R the radius of the bead. The diffusion constant then reads as $D = k_B T/\gamma$. The stiffness κ has an explicit dependence on time and $\xi(t)$ is a white Gaussian noise with autocorrelation $\langle \xi(t)\xi(t+t') \rangle = 2\delta(t')$. Equation (1) is overdamped (there is no acceleration term in $\ddot{x}$), which is fully justified for colloidal objects[30]. The Langevin description equation (1) can be recast into the following Fokker–Planck equation for the probability density[31]:

$$\partial_t \rho(x,t) = \partial_x \left[\frac{\kappa}{\gamma} x \rho \right] + D \partial_{xx}^2 \rho \tag{2}$$

At initial and final times (t_i and t_f), $\rho(x,t)$ is Gaussian, as required by equilibrium. A remarkable feature of the ESE (non-equilibrium) solution is that, for intermediate times, $\rho(x,t)$ remains Gaussian,

$$\rho(x,t) = \sqrt{\frac{\alpha(t)}{\pi}} \exp\left[-\alpha(t) x^2 \right] \tag{3}$$

We demand that

$$\alpha(0) = \frac{\kappa_i}{2k_B T} \quad \text{and} \quad \alpha(t_f) = \frac{\kappa_f}{2k_B T} \tag{4}$$

Combining equation (2) with equation (3), we obtain

$$\left[\frac{\dot{\alpha}}{2\alpha} - \dot{\alpha} x^2 \right] \rho = \frac{\kappa}{\gamma} \left(1 - 2\alpha x^2 \right) \rho - 2 \frac{k_B T}{\gamma} \alpha \left(1 - 2\alpha x^2 \right) \rho \tag{5}$$

Requiring that the equality holds for any position x, the equation is simplified into:

$$\frac{\dot{\alpha}}{\alpha} = \frac{2\kappa}{\gamma} - \frac{4 k_B T \alpha}{\gamma} \tag{6}$$

This relation was obtained in refs 23,24 by studying the evolution of the variance σ_x^2. However, unlike in these works, we supplement our description with the constraints $\dot{\alpha}(0) = \dot{\alpha}(t_f) = 0$, as a fingerprint of equilibrium for both $t < 0$ and $t > t_f$.

Next, the strategy goes as follows. We choose the time evolution of α, complying with the above boundary conditions. To this end, a simple polynomial dependence of degree 3 is sufficient. Other more complicated choices are also possible. Introducing the rescaled time $s = t/t_f$, we have

$$\alpha(s) = \frac{1}{2k_B T} \left[\kappa_i + \Delta\kappa (3s^2 - 2s^3) \right] \tag{7}$$

where $\Delta\kappa = \kappa_f - \kappa_i$. Finally, equation (6) has been satisfied, from which we infer the appropriate evolution $\kappa(t)$ that is then implemented in the experiment:

$$\kappa(t) = \frac{3\gamma \Delta\kappa\, s(1-s)/t_f}{\kappa_i + \Delta\kappa(3s^2 - 2s^3)} + \kappa_i + \Delta\kappa(3s^2 - 2s^3) \tag{8}$$

The analysis, restricted here to the one-dimensional problem, can be easily recast in three dimensions. It is also straightforward to generalize the idea to account for a time-dependent temperature $T(t)$, which can be realized experimentally[20]. In this latter situation, the key relation equation (6) is unaffected, and therefore indicates how κ should be chosen, for prescribed $\alpha(t)$ and $T(t)$. This highlights the robustness of the ESE protocol.

The mean work exchanged in the course of the transformation takes a simple form in our context:

$$\langle W \rangle = \int_0^{t_f} \frac{\langle x^2 \rangle}{2} \frac{\mathrm{d}\kappa}{\mathrm{d}t} \mathrm{d}t \tag{9}$$

According to our ansatz (3), $\langle x^2 \rangle = 1/(2\alpha(t))$, and using the relation (6), equation (9) can be written in the following form[23,24]:

$$\langle W \rangle = \int_0^{t_f} \frac{1}{4\alpha} \frac{\mathrm{d}\kappa}{\mathrm{d}t} \mathrm{d}t = \int_0^{t_f} \frac{\kappa}{4} \frac{\dot{\alpha}}{\alpha^2} \mathrm{d}t = \frac{k_B T}{2} \log\left(\frac{\kappa_f}{\kappa_i} \right) + k_B T \frac{\tau_{\mathrm{relax}}}{t_f} \left(\frac{\kappa_f}{\kappa_i} \right) \eta \tag{10}$$

where $\tau_{\mathrm{relax}} = \gamma/\kappa_f$ and η is a numerical factor given by

$$\eta = \frac{\alpha_i}{4} \int_0^1 \frac{1}{\alpha^3} \left(\frac{\mathrm{d}\alpha}{\mathrm{d}s} \right)^2 \mathrm{d}s = 9 \left(\frac{\Delta\kappa}{\kappa_i} \right)^2 \int_0^1 \frac{s^2(1-s)^2}{(1 + (\Delta\kappa/\kappa_i)(3s^2 - 2s^3))^3} \mathrm{d}s \tag{11}$$

Notice that equation (10) coincides with expressions derived in previous works[32,33] using linear response theory.

For our parameters, we find $\eta \simeq 0.106$, as indicated in the main text. Interestingly, expression (10) gives the free energy difference value in the limit $t_f \gg \tau_{\mathrm{relax}}$, $0.5 k_B T \log(\kappa_f/\kappa_i)$, which appears as the minimal mean work. In the opposite limit, we have a time–energy relation: $t_f \langle W \rangle = k_B T \tau_{\mathrm{relax}} (\kappa_f/\kappa_i)\eta$. We emphasize that the scaling in $1/t_f$ when $t_f \to 0$ is ansatz independent, although the specific value of the η parameter depends on the ansatz. It can be shown that the lowest η value for all admissible protocols is $(\sqrt{\kappa_i/\kappa_f} - 1)^2$, which gives $3/2 - \sqrt{2} \simeq 0.086$ here. Thus, our protocol, although sub-optimal in terms of mean work, nevertheless has an η value close to the best achievable.

Data availability. The data that support the plots within this paper and other findings of this study are available from the corresponding author on request.

References

30. Barrat, J.-L. & Hansen, J.-P. *Basic Concepts for Simple and Complex Liquids* (Cambridge Univ. Press, 2003).
31. Risken, H. *The Fokker-Planck Equation* (Springer, 1984).
32. Sivak, D. A. & Crooks, G. E. Thermodynamic metrics and optimal paths. *Phys. Rev. Lett.* **108,** 190602 (2012).
33. Bonança, M. & Deffner, S. Optimal driving of isothermal processes close to equilibrium. *J. Chem. Phys.* **140,** 244119 (2014).